Noise Performance of a Phased-Array Feed Composed of Thick Vivaldi Elements with Embedded Low-Noise Amplifiers

B. Veidt[*1], *T. Burgess*[1], *K. Yeung*[2], *S. Claude*[2], *I. Wevers*[2], *M. Halman*[2], *P. Niranjanan*[2], *C. Yao*[2], *A. Jew*[2], *D. Henke*[2], *A. G. Willis*[1]

[1]NRC Herzberg, Box 248, Penticton, BC V2A 6J9 Canada, email: bruce.veidt@nrc.ca
[2]NRC Herzberg, 5071 West Saanich Road, Victoria BC V9E 2E7 Canada

Abstract

Phased-array feeds (PAFs) can provide multi-beam capability for microwave reflector antennas. For radio astronomy applications it is crucial that the effective noise temperature of the PAF system be as low as practicable to be competitive with more conventional optimised single-beam systems. We describe our efforts to reduce the noise by using thick metal Vivaldi elements to reduce resistive losses, minimizing use of dielectrics to reduce dielectric losses, and embedding the LNA circuitry within the thick element as close to the feed point as possible. To demonstrate these improvements a 41-element array has been constructed with an analogue beamformer to combine the central 9 elements. Y-factor measurements using free-space hot and cold loads show a minimum array noise temperature of less than 35K.

1 Introduction

Traditionally radio astronomy has been dominated by telescopes with single beams. Over the last decade, however, phased-array feeds (PAFs) have demonstrated multi-beam operation on reflector antennas [1, 2, 3, 4]. The key advantage of increasing the number of beams per unit collecting area is an increase in the speed of the telescope when performing large-area surveys. Survey speed is a key design parameter for future telescopes such as the Square Kilometre Array (SKA) [5], and is proportional to $\Omega \left(A_{eff}/T_{sys}\right)^2$ where A_{eff} is the effective aperture area, T_{sys} is the telescope system temperature, and Ω is the solid angle of the instantaneous field of view. This equation shows that it is not sufficient to simply increase Ω, the system temperature must also be kept low.

Most PAFs to date employ ambient-temperature low-noise amplifiers (LNAs) because it is difficult to cool large systems to cryogenic temperatures. Although T_{min} for both commercial and experimental LNAs is as low as 14–21K [6], realised arrays have had noise temperatures much higher than this [7, 8]. This paper will report an experimental investigation into improving the noise performance of an array through reduction of dissipative losses .

2 Element Design

The purpose of the experimental array is to demonstrate low noise performance suitable for use as a focal-plane array on reflector antennas. This array, known as the Advanced Focal Array Demonstrator (AFAD), is based on Vivaldi elements [9]. These elements have been modified to reduce loss in the following ways: 1) Elements are made from 5 mm solid metal instead of printed circuit boards [9] or sheet metal [10]. This change increases the area over which slot line currents flow, reducing the current density and thereby reducing resistive loss. A small loss, such as 0.1 dB, introduces significant noise ($\sim$7K). 2) Thick elements are free-standing without the need of a supporting dielectric substrate (as in printed circuit boards), eliminating most dielectric losses. 3) Thick Vivaldi elements allow the LNA to be embedded within the element very close to the feed point, eliminating input transmission line losses.

The Vivaldi element design is described elsewhere [11, 12]. Parameters describing the element geometry (taper length, slotline width, thickness, backshort diameter) are optimised for an LNA $Z_{opt} \approx 85\Omega$ measured for Avago MGA16516 ICs [personal communication, L. Belostotski, 2009]. Array s-parameters were then used to predict the array performance using methods described in [8]. Table 1 summarises AFAD design parameters, Fig. 1 shows a single element, and Fig. 2 shows a complete 41-element array.

3 Test Array

The test array consists of 41 elements, arranged in 2 polarizations. An analogue beamformer combines 9 central elements in one polarisation to form a single broadside beam. The beamformer consists of three 4-way combiners, step attenuators for beamforming weight adjustment, and sufficient gain so that beamformer loss does not degrade noise performance. By symmetry, groups of elements can be controlled by a single attenuator [13]. All channels through the beamformer have been made as similar as possible to ensure phase tracking with physical temperature, weight setting, and frequency. Output power was measure with a Rohde and Schwarz FSL18 spectrum analyser.

978-1-4673-5225-3/14/$31.00

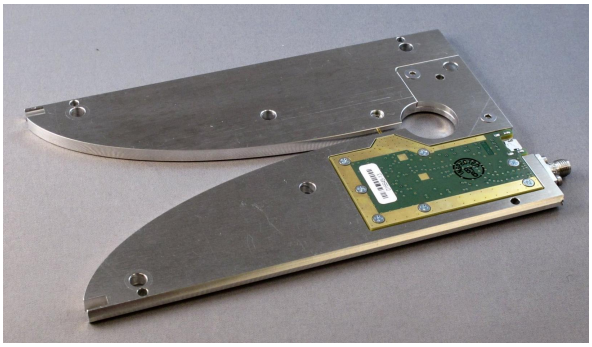

Figure 1: A single thick Vivaldi element with LNA installed. LNA components are on the underside of the green printed-circuit board. Each element was milled in two pieces which were then aligned with dowel pins and secured with fasteners. Coupling from the slotline to the LNA is accomplished by a pin that extends across the slot.

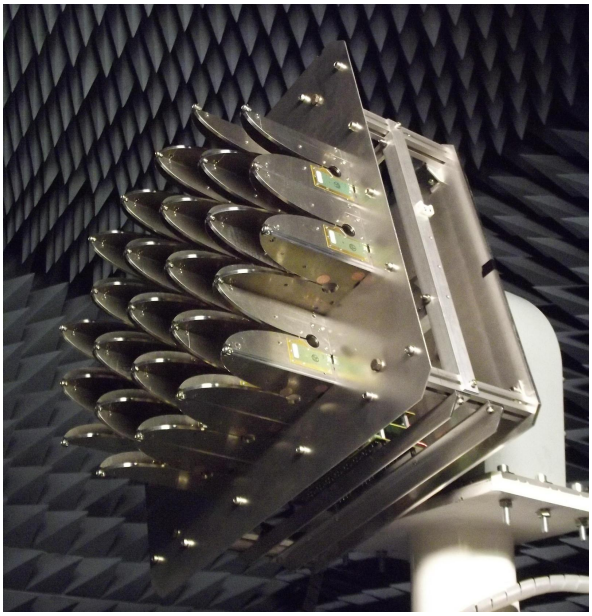

Figure 2: The complete AFAD 41-element thick Vivaldi array in an anechoic chamber. The analogue beamformer is located in the frame structure behind the ground plane.

4 Noise Measurement System

Noise characterisation of the array uses the Y-factor method with the sky as the cold load and ambient absorber as hot load. To reduce contamination by ground radiation, the array is placed at the bottom of a metallic shielding structure with the opening facing the zenith, shown in Fig. 3. With the roof closed, thermal radiation from the absorber reflects off the shield structure, embedding the test array in an ambient-temperature radiation field.

The system temperature is calculated using

$$T_{sys} = (T_H - Y T_C) / (Y - 1) \tag{1}$$

where T_C is the cold load physical temperature, T_H is the hot load temperature, and Y is the ratio of output powers with hot and cold loads at the input. The sensitivity to errors in Y, T_C, and T_H can be found by taking partial derivatives and inserting typical values, yielding these values:

$$\begin{aligned} \Delta T_{sys} &\sim 0.1 \cdot \Delta T_H \\ \Delta T_{sys} &\sim \Delta T_C \\ \Delta T_{sys} &\sim 5 \cdot \Delta Y \end{aligned} \quad . \tag{2}$$

This shows that the uncertainty in T_H is much less significant than the uncertainties due to T_C and Y. Uncertainty in Y is controlled by careful measurement technique. Uncertainty in T_C is reduced by using an accurate model of the sky.

There are three components to T_C: the Cosmic Microwave Background (2.7K), the atmosphere ($\sim$ 2K) [14], and diffuse galactic emission. The Global Sky Model package [15] was used to produce all-sky maps of galactic radio emission at relevant frequencies which are convolved with Gaussian beams to approximate the array beam.

Table 1: AFAD Design Parameters

Frequency range	0.7–1.5 GHz	Slot width	3 mm
Element spacing	100 mm	Overall length	158 mm
Element thickness	5 mm	Number of elements	41
Taper length	113 mm		

Figure 3: Hot/Cold Test Facility for measuring receiving system noise performance. The test chamber on the right side consists of a metallic ground shield covered with a roof with microwave absorber (hot load) on the underside. The opening is 4.1 m × 4.1 m and the slope of the walls is 25° from vertical. The roof can be moved along the elevated tracks, exposing the test system to cold sky. The structure on the left contains the test equipment.

5 Results

Typical results are shown here for measurements taken on 19 November, 2014 at 15:15 PST. The beamformer was adjusted to combine nine central elements with equal weight. The spectrum analyser was set to a resolution bandwidth of 3 MHz. The output data has 501 frequency points and is the average of 16 scans. The physical temperature of the absorber (6.5°C) was measured with an infrared thermometer. The galactic contribution to T_C was estimated to be 3.7K. The time interval between hot and cold measurements was 6 minutes, an interval short enough that electronic drifts were insignificant.

The output spectra for hot and cold loads are shown in Fig. 4a. Terrestrial (0.85–0.9 GHz) and satellite (1.15–1.3 GHz) interference are visible in the cold scan, which had the absorber roof removed. The signal power of the interference is a small fraction of the overall band so it does not affect the linearity of the system.

The system temperature of the array can be derived from these measurements using (1) and assuming $T_H = 273 + 6.5 = 279.5$K and T_C consisting of a Cosmic Microwave Background component (2.7K), a galactic component (3.7K), and a component due to atmospheric absorption (2K) for a total of 8.4K. Fig. 4b shows that the minimum noise temperature of the array is less than 35K.

6 Discussion and Conclusions

We have demonstrated an integrated low-noise phased-array element. The antenna element is a Vivaldi type and constructed of 5-mm thick aluminum which provides a larger surface area for surface currents to flow thereby reducing loss. This construction also permits the LNA to be embedded inside the element, placing the input very close to the feed point to reduce feed-line loss. Using free-space hot and cold loads we measure an array noise temperature less than 35K.

Future efforts will focus on increasing the useful bandwidth of the array by improving the noise match. This can be achieved by adjusting the input circuitry of the LNA and by increasing the element thickness to reduce the source impedance presented to the LNAs [16].

References

[1] D. R. DeBoer, R. G. Gough, J. D. Bunton, T. J. Cornwell, R. J. Beresford, S. Johnston, *et al.*, "Australian SKA Pathfinder: A high-dynamic range wide-field of view survey telescope," *Proc. IEEE*, vol. 97, pp. 1507–1521, 2009.

[2] W. van Cappellen and L. Bakker, "Initial results of the digital focal plane array demonstrator for APERTIF," in *Deep Surveys of the Radio Universe with SKA Pathfinders*, Univ. Western Australia, 2008.

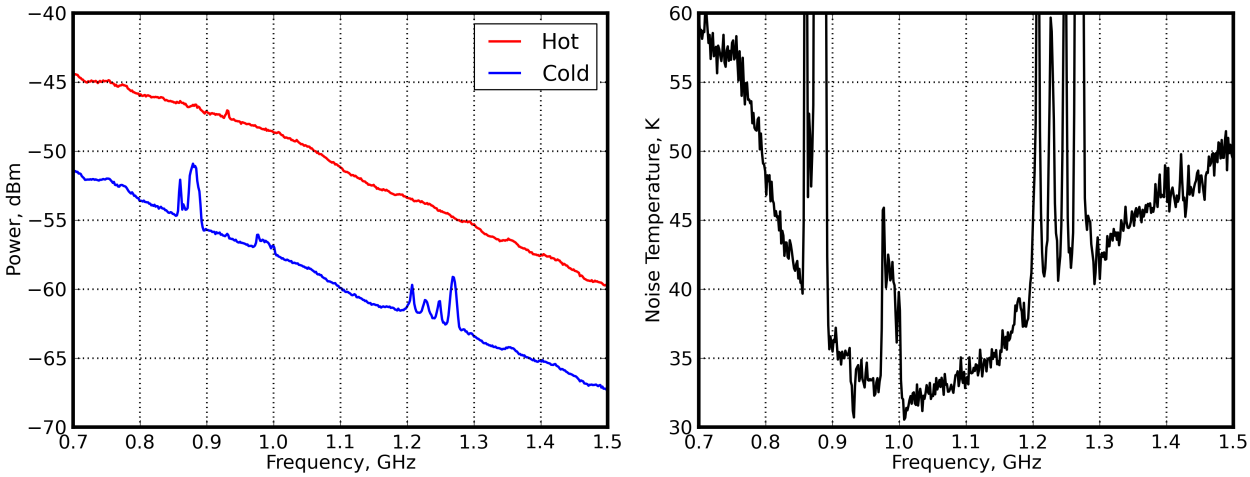

(a) Output spectra of the AFAD array.

(b) Noise temperature of the AFAD array.

Figure 4: (a) The upper trace shows the output signal with the absorber roof in place (hot measurement) and the lower trace shows the output with the absorber removed and the array exposed to cold sky. (b) Hot and cold measurements were used to generate this plot. Vertical displacements at 0.85–0.9, 0.93, 0.97–1.0, 11.9, and 1.15–1.3 GHz are due to radio-frequency interference.

[3] K. F. Warnick, B. D. Jeffs, J. Landon, J. Waldron, D. Jones, A. Stemmons, *et al.*, "BYU/NRAO 2007 Green Bank 20 meter focal plane array – Modeling and experimental results." SKADS MCCT Technical Workshop 'Design of Wideband Receiving Array Systems', 26–30 November 2007.

[4] B. Veidt, G. Hovey, T. Burgess, R. Smegal, R. Messing, A. G. Willis, *et al.*, "Demonstration of a dual-polarized phased-array feed," *IEEE Trans. Antennas Propag.*, vol. 59, pp. 2047–2057, 2011.

[5] P. E. Dewdney, P. J. Hall, R. T. Schilizzi, and T. J. W. Lazio, "The Square Kilometre Array," *Proc. IEEE*, vol. 97, pp. 1482–1496, 2009.

[6] L. Belostotski and J. Haslett, "Evaluation of tuner-based noise-parameter extraction methods for very low noise amplifiers," *IEEE Trans. Microw. Theory Techn.*, vol. 58, pp. 236–250, 2010.

[7] W. van Cappellen, J. G. B. de Vaate, K. Warnick, B. Veidt, R. Gough, C. Jackson, and N. Roddis, "Phased array feeds for the Square Kilometre Array," in *Proc. XXXth URSI General Assembly and Scientific Symp*, pp. 1–4, 2011.

[8] K. F. Warnick, D. Carter, T. Webb, J. Landon, M. Elmer, and B. D. Jeffs, "Design and characterization of an active impedance matched low-noise phased array feed," *IEEE Trans. Antennas Propag.*, vol. 59, pp. 1876–1885, 2011.

[9] H. Holter, T.-H. Chio, and D. H. Schaubert, "Experimental results of 144-element dual-polarized endfire tapered-slot phased arrays," *IEEE Trans. Microw. Theory Techn.*, vol. 48, pp. 1707–1718, 2000.

[10] A. van Ardenne, J. Bregman, W. van Cappellen, G. Kant, and J. Bij de Vaate, "Extending the field of view with phased array techniques: Results of European SKA research," *Proc. IEEE*, vol. 97, pp. 1531–1542, 2009.

[11] R. Sarkis, C. Craeye, and B. Veidt, "Thick Vivaldi antenna for focal plane applications," in *Proc. IEEE Int. Antennas and Propagation (APS-URSI) Symp.*, pp. 1988–1991, 2011.

[12] R. Sarkis, B. Veidt, and C. Craeye, "Fast numerical method for Focal Plane Array simulation of 3D Vivaldi antennas," in *Int. Conf. on Electromagnetics in Advanced Applications (ICEAA)*, pp. 772–775, 2012.

[13] M. Ivashina and J. Bregman, "Experimental synthesis of a feed pattern with a dense focal plane array," *European Microwave Conference*, 2002.

[14] J. A. Allnutt, *Satellite-to-Ground Radiowave Propagation*. London, UK: Peter Peregrinus, 1989.

[15] A. De Oliveira-Costa, M. Tegmark, B. M. Gaensler, J. Jonas, T. L. Landecker, and P. Reich, "A model of diffuse Galactic radio emission from 10 MHz to 100 GHz," *Monthly Notices of the Royal Astronomical Society*, vol. 388, pp. 247–260, 2008.

[16] R. Sarkis, *Antenna Arrays for Direction of Arrival Estimation and Imaging*. PhD thesis, Université catholique de Louvain, 2011.